

## Assessment of brain injury biomechanics in soccer heading using finite element analysis

Richard A. Perkins<sup>a</sup>, Amirhamed Bakhtiarydavijani<sup>b,\*</sup>, Athena E. Ivanoff<sup>a</sup>, Michael Jones<sup>d</sup>, Youssef Hammi<sup>b,c</sup>, Raj K. Prabhu<sup>a</sup>

<sup>a</sup> Universities Space Research Association, Cleveland, OH, United States of America

<sup>b</sup> Center for Advanced Vehicular Systems, Mississippi State University, Starkville, MS, United States of America

<sup>c</sup> Department of Mechanical Engineering, Mississippi State University, Starkville, MS, United States of America

<sup>d</sup> Institute of Medical Engineering & Medical Physics, Cardiff University, Cardiff, Wales, United Kingdom

### ARTICLE INFO

#### Keywords:

Finite element  
Soccer headings  
Mild traumatic brain injury  
Injury mechanics  
Biomechanical analysis

### ABSTRACT

This study presents an *in silico* finite element (FE) model-based biomechanical analysis of brain injury metrics and associated risks of a soccer ball impact to the head for aware and unaware athletes, considering ball impact velocity and direction. The analysis presented herein implements a validated soccer ball and 50<sup>th</sup> percentile human head computational FE model for quantifying traumatic brain injury (TBI) metrics. The brain's mechanical properties are designated using a viscoelastic-viscoplastic constitutive material model for the white and gray matter within the human head FE model. FE results show a dynamic human head-soccer ball peak contact area of approximately seven times greater than those documented for helmet-to-helmet hits in American Football. Due to the deformable nature of the soccer ball, the impact dynamics are unique depending on the location and velocity of impact. TBI injury risks also depend on the location of impact and the impact velocity. Impacts to the rear (BrIC:0.48, HIC<sub>15</sub>:180.7), side (BrIC:0.52, HIC<sub>15</sub>:176.5), and front (BrIC:0.37, HIC<sub>15</sub>:129.0) are associated with the highest injury risks. Furthermore, the FE results indicate when an athlete is aware of an incoming ball, HIC<sub>15</sub>-based Abbreviated Injury Scale 1 (AIS 1) injury risks for the front, side, and rear impacts decrease from 10.5%, 18.5%, and 19.3%, respectively, to approximately 1% in front and side impacts and under 6% in a rear impact. Lastly, the unique contact area between the head and soccer ball produces pressure gradients in the ball that translate into distinguishable stress waves in the skull and the cerebral cortex.

### 1. Introduction

Throughout the world, soccer is enjoyed by athletes of all ages at various levels of play proficiency. It has been reported approximately 265 million athletes worldwide participate in the game of soccer [1]. Some athletes begin playing soccer as early as six years of age, when neurological development is at a profound stage [2]. It has been reported for sports related concussions, soccer accounts for approximately 37%, combined for both men's and women's sports [3]. Additionally, soccer ball headings have been shown in one study may produce peak head accelerations 160 – 180% greater than those seen in noninjuries football (American) or hockey impacts [4] related head impacts. It has also been reported that concussions are responsible for 5.8% of all injuries during a men's soccer game [5] and 8.6% of all injuries in females [6] over 15-year duration. Interestingly, the goal keeper position

remains most prone to concussive injuries with 80% reported to have sustained at least one concussion during their career [7]. Studies indicate approximately 62% of soccer athletes experienced a concussion during their career; and, statistics reveal that only 20% of athletes realize and acknowledge a concussion has been sustained [8]. This suggests that some athletes may continue to play while concussed, leaving them vulnerable to further neurological impairment. It is noteworthy that most studies neglect to indicate the true causation of the concussion, such as player to player contact; or, player to ball contact. However, in response to the reported concussions, research groups are thoroughly investigating the effects and concerns related to repeated impacts in soccer players [9].

Presentation of chronic traumatic encephalopathy (CTE) has been seen to occur after repeated head trauma and is characterized by progressive neurological degeneration [10]. Significant research aims to

\* Corresponding author at: Research Engineer II, Center for Advanced Vehicular Systems, 200 Research.

E-mail address: [hamed@cavs.msstate.edu](mailto:hamed@cavs.msstate.edu) (A. Bakhtiarydavijani).

investigate the correlation between CTE and repeated brain trauma, including head impacts that result in symptoms inferior to the threshold associated with the diagnosis of a concussion [11]. Common symptoms of concussions consist of headaches, nausea, fatigue, and possible changes in vision, especially diplopia (or, double vision). Since common soccer techniques, such as heading a soccer ball, are rarely reported, to acknowledge these concussive symptoms, other areas of neurological impairment have drawn interest from researchers. Head impacts have been known to affect an individual's neurological functioning, such as memory and planning capabilities. A solid correlation has been established [12] indicating repeated exposure to soccer competitions often heightened deterioration of memory and planning capabilities, determined by psycho-neurological testing and evaluation.

FE soccer ball models have previously been developed to accurately represent the behavior of a FIFA regulation size soccer ball (size 5) [13, 14]. There are limited numerical studies which focus on the relationship between the location of impact on the players head and corresponding risk of injury. One particular study utilizes a finite element analysis (FEA) approach to examine the results of heading a soccer ball on the forehead or on top of a player's head with the possible occurrence of a mild TBI [15]. Additionally, head to ball contacts in soccer have been shown to cause concussion [16]. It has also been indicated that soccer headings independently contribute to cognitive impairment [17]. Particularly, a heightened risk of injury is caused by impact to the forehead and temple of the head, rather than the occiput region of the head [16,18]. Since soccer ball headings frequently occur during a match, the forehead region (including the scalp and supraorbital ridge) is frequently subjected to impact by the soccer ball. For this reason, great interest exists to understand the risk of injury associated with this technique. Research has evaluated the effects of a single ball to head impact by assessing the soccer ball at velocities between 10 and 30 m/s on a Hybrid III test dummy [18]. Using the Head Injury Power (HIP), injury criteria, results indicate a singular impact from a soccer ball poses less than a five percent risk of resulting in concussive symptoms [18]. However, other studies suggest that a soccer ball striking a player's head is associated with significant neurological injuries, such as a large chronic and/or subacute subdural hematoma [19]. Finally, repeated impacts to a player's head region have been correlated to reduced brain function regarding memory consolidation, planning ability, and mental dexterity [20,21].

During active heading of a soccer ball, the player anticipates contact with the ball, which cause the neck muscles to tense in preparation for stabilizing the head and neck. Most heading related concussions occur when a player is not expecting contact with the incoming soccer ball as opposed to a player purposefully heading the ball [22]. When a soccer player is intentionally heading a soccer ball, activated neck muscles limit the movement of the player's head. As the strength of the neck increases, the athlete can better control and reduce the movement of the head and thus, mitigate the severity of injury [23–26]. Conversely, if the player is not expecting to achieve contact with the soccer ball using their head, the neck region fails to limit motion of the head in the same prospective manner; thus, increasing the kinematic range of movement of the head. In turn, increasing the likelihood and probability of injury due to soccer ball headings.

In the present study, a finite element (FE) model consisting of a human head and soccer ball is developed to evaluate head injury risk, severity, and mechanisms associated with heading a soccer ball. Using this FE model, this study investigates the effects of the impact location, impact velocity, and an active or passive neck condition during headings by soccer athletes.

## 2. Methods

### 2.1. Finite element model development

Herein, an FE model of a size 5 regulation-size soccer ball (FIFA) is

developed to conduct impact simulations with a previously developed 50<sup>th</sup> percentile human head to study the impact caused by heading a soccer ball. The dimensions and density measurements of the soccer ball are extrapolated from the literature [13] and are defined as a spherical shape with a diameter of 220 mm. The ball consists of two layers, an inner latex bladder layer and an outer shell layer. The inner layer has a thickness of 0.8 mm and a density of 1175 kg/m<sup>3</sup>; the outer shell has a thickness of 2.2 mm and a density of 900 kg/m<sup>3</sup>. Mechanical testing of the soccer ball was conducted through uniaxial tensile testing [27] and the experimental data is used to define a reduced polynomial strain energy equation. This serves as an acceptable, hyperelastic model, considering its coefficients could be well defined by this type of experiment. The reduced polynomial strain energy potential equation is shown by Eq. .

$$U = \sum_{i=1}^N C_{i0} (\bar{I}_1 - 3)^i + \sum_{i=1}^N \frac{1}{D_i} (J^{el} - 1)^{2i} \quad (1)$$

In Eq. 1,  $C_{i0}$  and  $D_i$  are material constants,  $\bar{I}_1$  is the first strain invariant,  $J^{el}$  is the elastic volume ratio and  $U$  represents the strain energy per unit of reference volume. The soccer ball is assumed to be fully incompressible; therefore, the  $D_i$  material constants are set to 0. The inner latex bladder layer and the outer shell layer are characterized using a fourth order and fifth-order polynomial strain energy potential, respectively. To model the viscous material properties of the soccer ball, a proportional damping stiffness ( $\beta_R$ ) coefficient is defined in the outer panel material model. This damping is introduced in proportion to the strain rate, which is similar to defining viscous material damping. Thus, creating an additional damping stress, ( $\sigma_d$ ) proportional to the total strain as seen in Eq. 2 where  $D^{el}$  is the material's current elastic stiffness and  $\epsilon$  represents strain rate.

$$\sigma_d = \beta_R D^{el} \epsilon \quad (2)$$

The value of the proportional damping stiffness is determined by an iterative process and observation of the results of the ball's verification simulations. The value of the damping stiffness that best fits the comparison data is determined to be 0.00025. The ball's mesh is designed using shell elements, since the thickness of the ball is less significant in comparison to the other dimensions of the soccer ball.

Prior to any soccer ball being used in a game, it must be inflated to a specified pressure. A ball pressure of 0.09 MPa lies within the pressure range used for regulation soccer games [28] and is implemented for these simulations. This value also represents an approximate mean of the allowable pressure ranges and has been used in previous studies for developing FE models of a regulation soccer ball [13,27]. To represent the air pressure, a surface fluid-based cavity technique is defined for the analysis. This is accomplished by coupling a cavity reference node at the center of gravity of the soccer ball to its inner surface. To define the air in the ball, the molecular weight is defined as 0.02897  $\frac{kg}{mol}$ . Additionally, since this study is performed using an explicit analysis, the heat capacity ( $C_p$ ) is required. This is achieved by applying the polynomial form of heat capacity, as shown by Eq. 3, where  $\tilde{a}$ ,  $\tilde{b}$ ,  $\tilde{c}$ ,  $\tilde{d}$ , and  $\tilde{e}$  are gas constants,  $\theta$  is the current temperature, and  $\theta^z$  represents temperature of absolute zero (0).

$$\tilde{C}_p = \tilde{a} + \tilde{b}(\theta - \theta^z) + \tilde{c}(\theta - \theta^z)^2 + \tilde{d}(\theta - \theta^z)^3 + \frac{\tilde{e}}{(\theta - \theta^z)^2} \quad (3)$$

The calibrated stress-strain curves for the inner latex bladder layer and the outer shell layer defined by the hyperelastic material model are shown in Supplemental Fig. 1. The material constants described in this definition, as well as the hyperelastic material definition, are delineated in Table 1. To allow for gradual inflation of the soccer ball, an inflation step is defined for 1ms, to enable the soccer ball to achieve a state of equilibrium prior to the impact simulation. This prevented any distortion of elements caused by rapid expansion of the ball.

**Table 1**

Soccer ball hyperelastic material constants, heat capacity of air constants used in the soccer ball finite element model, and the body moment of inertia.

inner bladder (MPa)	Outer panel (MPa)	heat capacity	Moment of inertia (N·m <sup>2</sup> )
C <sub>10</sub> 0.12	C <sub>10</sub> 12.4	$\tilde{a}$ 28.110 (J/mol·K)	I <sub>11</sub> 13.56
C <sub>20</sub> 0.17	C <sub>20</sub> -24.5	$\tilde{b}$ 1.967e-3 (J/mol·K <sup>2</sup> )	I <sub>22</sub> 14.28
C <sub>30</sub> -0.24	C <sub>30</sub> 84.1	$\tilde{c}$ 4.802e-6 (J/mol·K <sup>3</sup> )	I <sub>33</sub> 1.42
C <sub>40</sub> 0.14	C <sub>40</sub> -126.0	$\tilde{d}$ -1.966e-9 (J/mol·K <sup>4</sup> )	
	C <sub>50</sub> 72.0	$\tilde{e}$ 0.0 (J/mol·K <sup>5</sup> )	

## 2.2. Soccer ball model validation

To ensure that the FE soccer ball appropriately modeled the behavior of a FIFA regulation size 5 soccer ball used for regulation games, the ball is verified by simulations of the soccer ball impacting a rigid wall. The results are compared with experimental data [27]. To model the contact between the ball and the plate, a surface-to-surface contact is used with a hard contact pressure overclosure relationship. Impact velocities for verification included 11, 15, 20, 22 and 28 m/s.

The validation criteria are defined by considering the maximum displacement of the soccer ball, the contact time with the wall, and the coefficient of restitution. The coefficient of restitution is defined as the ratio of the exit velocity of the soccer ball to its initial velocity. This validation study is conducted using these three criteria and are compared to the experimental data (Supplemental Fig. 2). It is shown that the FE model of the soccer ball resembled the actual behavior of a regulation size ball during experimental testing.

Additionally, to determine the optimal number of elements required to represent the response of the soccer ball, a mesh convergence study is performed. This is accomplished by simulating a soccer ball with an initial velocity of 20 m/s impacting a rigid wall at different mesh densities; in which duplicate criteria as the validation study is considered. It is evident that at approximately 3,000 elements, minimal changes to the response exist (Supplemental Fig. 2). This number also serves the interest of minimizing the computational time, maximizing cost efficiency of the simulations and, therefore, is adopted as the specified mesh density.

## 2.3. Human head FE model description and validation

The human head model represents a 50th-percentile male athlete and includes distinct representations of the scalp, cranium (skull), cerebral spinal fluid (CSF) and the brain. The entire FE head model consists of 1,248,377 elements. A viscoelastic-viscoplastic material model defines the gray and white matter of the brain. Its mechanical behavior is captured using a validated internal state variable (ISV) model, calibrated for intermediate to high strain rates [29,30]. The FE head model's development and formulation are further discussed in [31]. The response of the head was validated by the coup and countercoup pressure histories, produced by postmortem human subject (PMHS) experiments [32] and compared to simulation data [31], with good agreement (Supplemental Fig. 3). Additionally, the FE head model is validated for relative brain-skull displacements for the case C383-T1 presented in [33]. The experimental data presented used neutral density targets (NTD) implanted into the brain of the PMHS at various locations to determine their displacements relative to the skull at these specific locations. Similarly, nodes are selected in the FE head model, which are closest to the experimental locations of the NTDs. The nodes' relative displacements are calculated and compared with the experimental data to validate the head response for this study (Supplemental Fig. 4).

## 2.4. Finite element simulation design

The finite element simulations are designed and completed using the software package Abaqus (Dassault Systemes, 2019). The experimental set up is designed to account for three input variables: ball velocity, impact location, and the anticipation by the player of the incoming ball. These simulations incorporate a nonstructural mass and moment of inertia in its design. Eq. 4 presents the relationship that enables the center of gravity of the human body to be determined based on a player's height and weight [34]. The mass moment of inertia, shown in Table 1, is specified based on prior published data [35] determined from volunteers. The body nonstructural mass and moment of inertia are assigned to the center of gravity of the body (RF1). A second massless point (RF2) is defined 1 cm below the base of the spine in the FE model to account for a relaxed or locked neck (Fig. 1).

$$COG = (h \times 0.597 + w \times 0.16 - 5.82) \quad (4)$$

The anticipation of the ball by the player is accounted for by two conditions: an active or a passive neck condition. As discussed previously, when a player is expecting and preparing for an incoming ball, the player's stabilizing neck muscles will tense. This is considered to be the active neck condition. To model this scenario, RF2 to RF1 and base vertebra elements to RF2 are coupled for displacement and rotations (Fig. 1b). If the player is not anticipating the incoming ball the passive neck condition is assumed. The scenario is modeled by, coupled displacement and rotations for RF2 to RF1 and coupled displacement with free rotational degrees of freedom for the base vertebra elements to RF1 (Fig. 1a). Hence, the active neck condition will limit the head movement relative to the athlete's body while the passive neck condition will allow head rotations about the spine base.

Rotational velocities and accelerations are important measurements for certain injury metrics; however, traditional three-dimensional (3-D) elements lack rotational degrees of freedom and are unable to calculate the rotational components. To account for the rotational components, rotational accelerometer connector elements are assigned at the center of gravity of the head, and at 2.5 cm away from this point along the x, y, and z directions, conceptually similar to previous studies [36]. The soccer ball's path is assigned along an axis of impact, which is defined by the ball's center of gravity and the center of gravity of the brain of the human head. Ball-head impacts occurring during a soccer game consist of a range of velocities. Previous studies have shown peak ball velocities resulting from a player's kick ranging from approximately 24 m/s – 34 m/s depending on factors such as competition level, player position, or kick method [37–40]. Simulations of the soccer ball impacting the front, side (lateral), top and back of the human head at 35 m/s are

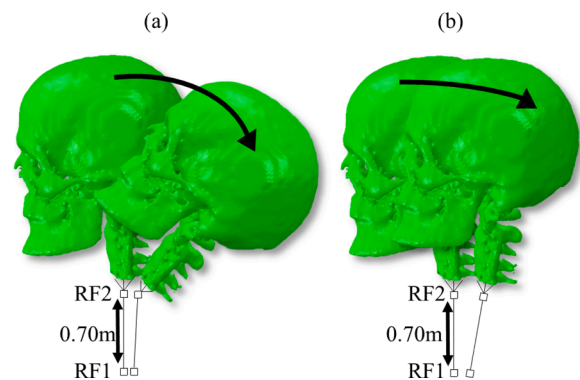


**Fig. 1.** Representation of the passive (a) and active (b) neck conditions used in the simulations. The arrows indicate the free rotation allowed in the passive neck condition and the constrained rotation implemented by the active condition due to the activation of the neck. Inertial mass and rotational inertia are applied to RF1 (center of gravity of the body) and RF1 and RF2 are coupled for displacement and rotation.

implemented to ascertain the significance of impact location at a heightened ball impact velocity. A better understanding as to the effect of the inbound soccer ball velocity is accomplished by designing simulations of the soccer ball impacting the front of the human head model at velocities of 11, 23, and 35 m/s to encompass a wider range of velocities, which are expected to be encountered during games. The severity of injury for each case is determined by considering the peak stress and strain values for the frontal, temporal, parietal, occipital lobes, and cerebellum in the brain as well as kinematic and strain-based injury metrics. The kinematic injury metrics are determined for each case by the HIC<sub>15</sub> and BrIC injury criteria. The HIC<sub>15</sub> formulation is based on the acceleration  $a(t)$  of the head and is defined by Eq. 5.

$$HIC = \max \left[ \frac{1}{t_2} \int_{t_1}^{t_2} a(t) dt \right]^{-2.5} (t_2 - t_1) \quad (5)$$

The variables  $t_1$  and  $t_2$  are comprised between  $[0, t]$ , where  $t$  is the time period of the analysis. Additionally, the maximum time interval between  $t_1$  and  $t_2$  is specified to be 15 ms for this criterion. Injury metrics are commonly presented as Abbreviated Injury Scale (AIS) injury probabilities to offer a clinical comparison of the data presented. AIS injury curves have been derived from existing safety standards for the criteria presented herein [41]. The BrIC is established by the head's rotational velocities and is defined according to Eq. 6 [42].

$$BrIC = \sqrt{\left(\frac{\omega_x}{66.25_{rad}}\right)^2 + \left(\frac{\omega_y}{56.45_{rad}}\right)^2 + \left(\frac{\omega_z}{42.87_{rad}}\right)^2} \quad (6)$$

A BrIC value of 0.5 has been shown to correlate to a 50% risk of a concussion and a value of approximately 0.53, using the maximum principal strain (MPS) criteria, indicates a 50% risk of AIS 2 injury [42]. Each simulation is run for 15 ms to capture the impact and rebound of the ball at the athlete's head. The results obtained from these simulations are essential to determine the risk of injury, severity, and their respective correlation, as the metrics described previously are calculated and compared against existing values in current literature. Various threshold values also exist for different injury predictors and injury severities. It has been proposed that HIC<sub>15</sub> values of 151 and 240 correspond to a 25 and 50% risk of a mild traumatic brain injury (mTBI), respectively [43]. The cumulative strain damage measure (CSDM) is a strain-based metric also calculated in these simulations. This metric calculates the percent of elements in the brain over a specified maximum principal strain threshold, which is set as 5% for this study. This metric and strain threshold has been used in previous studies when studying TBI [44].

### 3. Results

The FE simulations evaluate the effect of the soccer ball headings on brain injury and associated risks due to soccer ball impact location, impact velocity and the active versus passive heading of the soccer ball. The results of the simulations are evaluated by BrIC, HIC<sub>15</sub>, peak pressure, Von Mises stress, and max principal strain.

#### 3.1. Injury metrics predictions from finite element simulations

The HIC<sub>15</sub> and BrIC injury metrics calculated for soccer ball impacts to the front (anterior), top (superior), side (lateral), and rear (posterior) regions of an athlete's head, with an inbound soccer ball velocity of 35 m/s, are shown in Fig. 2a and b for both passive and active neck conditions. Additionally, the injury metrics are presented for frontal soccer ball impacts at inbound soccer ball velocities of 11 m/s, 23 m/s, and 35 m/s (Fig. 2c, d). Table 2 presents the peak values for pressure, Von Mises stress, and the maximum principal strain averaged for the frontal lobe, temporal lobe, parietal lobe, occipital lobe, cerebellum, and the full brain. Peak linear and angular acceleration of the head is also calculated

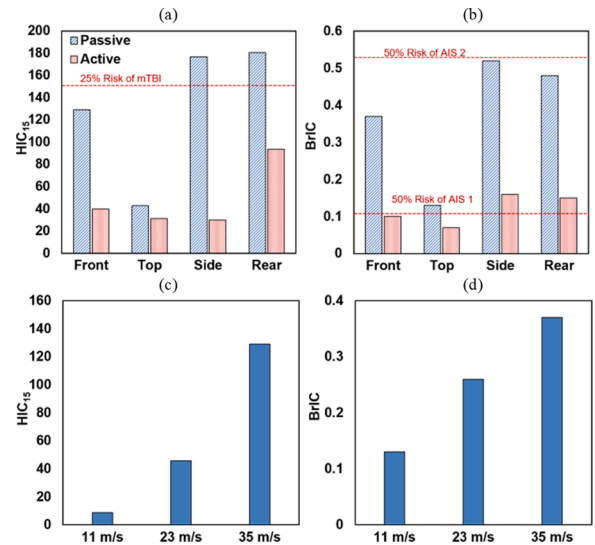


Fig. 2. Injury metric values for soccer ball headings at a 35 m/s ball velocity showing a comparison of active and passive headings at front, top, side, and rear impact locations using: (a) HIC<sub>15</sub>, and (b) BrIC. Shown also are the injury metric values for a passive frontal impact at 11 m/s, 23 m/s, and 35 m/s using: (c) HIC<sub>15</sub> and (d) BrIC.

from the simulations and is shown in Supplemental Table 1.

#### 3.2. Analysis of soccer ball-head contact area

The dynamic behavior of the contact area between the soccer ball and the player's head is shown in Fig. 3. The contact area appears to be directly proportional to the peak ball velocities. Additionally, the time interval between the initial and final contact remains independent of the ball peak velocity. The ball remains in contact with the head for approximately 12 ms, with the maximum contact occurring at approximately 6ms for each velocity tested. Additionally, the strain energy in the soccer ball is plotted in Fig. 4 for impact velocities of 35 m/s and 11 m/s in a passive frontal header.

#### 3.3. Brain response to soccer ball heading

The pressure evolution throughout the simulations is depicted by the contour plots provided in Figs. 5 and 6. Fig. 5 shows the pressure evolution for a frontal heading at 35 m/s for an active and passive neck condition; Fig. 6 exemplifies the pressure evolution due to a soccer heading at 35 m/s for various impact locations. The maximum compressive pressure at the coup site and the maximum tensile pressure at the countre-coup site are denoted in both figures. Additionally, Fig. 7 shows the time evolution of the maximum principal strain, pressure, and Von Mises stresses throughout the entire brain for a frontal impact with a passive neck condition.

#### 3.4. Stress wave propagation

Fig. 8 shows a frontal impact at a velocity of 35 m/s, a sagittal view of the initial propagation of stress waves - as depicted by pressure time evolution contour plots - through the brain for the passive and active neck conditions (Rows a and b) and an isometric view through the whole brain for the passive neck condition (Row c). The first and second stress waves that are captured in the simulation are shown to provide insight into the complex behavior of the dynamic stress interactions in the brain throughout the duration of the impact. Furthermore, Fig. 9 shows a sagittal view of the pressure evolution throughout the skull (Row a), and the soccer ball and the skull (Row b) to highlight the transmission of stress waves from the soccer ball to the head. Finally, Fig. 10 shows the

**Table 2** Peak values for pressure (P), Von Mises stress (VM), and maximum principal strain (MPS) in the frontal lobe, temporal lobe, parietal lobe, occipital lobe, cerebellum, and the full brain during a soccer ball heading for active and passive conditions at different soccer ball-head impact locations and a 35 m/s ball velocity (stress in units of kPa).

	Frontal			Temporal			Parietal			Occipital			Cerebellum			Full brain		
	P	VM	MPS ( $\times 10^{-3}$ )	P	VM	MPS ( $\times 10^{-3}$ )	P	VM	MPS ( $\times 10^{-3}$ )	P	VM	MPS ( $\times 10^{-3}$ )	P	VM	MPS ( $\times 10^{-3}$ )	P	VM	MPS ( $\times 10^{-3}$ )
<b>Front</b>	68.5	11.9	3.1	38.1	13.8	2.5	33.3	11.8	0.58	11.1	10.9	0.63	18.5	13.2	1.5	35.8	10.2	1.8
<b>Front<sub>Active</sub></b>	41.0	11.8	1.9	28.4	13.2	2.1	38.4	12.9	0.4	45.9	13.1	0.5	44.2	13.8	3.0	29.5	10.4	1.6
<b>Side</b>	40.1	14.2	35.3	19	14.1	39.4	40.1	14.4	52.6	40.2	15.1	48.7	42.2	14.2	57.3	47.3	11.1	44
<b>Side<sub>Active</sub></b>	41.3	14.5	16.7	28.7	14.5	20.3	36.3	14.5	20.3	40.3	14.7	20.4	40.7	15.3	25.7	34.5	11.5	19.0
<b>Top</b>	39.1	12.4	3.8	51	14.7	4.4	44.9	11.3	4.2	57.5	13.6	1.5	70.6	15.2	6.0	41.8	11.1	4.1
<b>Top<sub>Active</sub></b>	37.7	12.3	2.1	44.9	14.8	2.0	39.4	11.3	2.7	43.6	14.2	1.0	53.6	15.4	3.1	34.8	12.1	2.2
<b>Rear</b>	42.9	13.5	39.8	62.7	13.6	32.3	77.4	14.3	41.3	98.1	13	47.8	99.5	14.1	29.2	62.9	11.2	38
<b>Rear<sub>Active</sub></b>	60.9	13.5	5.5	41.6	13.8	8.7	56.9	14.3	5.3	83	13.1	7.9	55.1	13.9	6.9	34.9	11.0	6.6

peak values of the acceleration magnitude found in the soccer ball and the head. These peak values correlate to the outermost portion of the contact surface between the head and the soccer ball. The circular patterns arising from the contact surface are associated with the stress waves found in the brain coup site during impact (Fig. 8, Row c).

#### 4. Discussion

An FE model consisting of a human head and a soccer ball is developed to evaluate injury risk to the brain, and the mechanisms affiliated with heading a soccer ball. The input variables include soccer-athlete's head impact location, impact velocity, and active and passive neck condition during heading. The FE simulations provide insight of the injury risks associated with a soccer ball header, while accounting for the complex geometry and behavior of the brain.

##### 4.1. Impact severity for impact velocity and location

TBI metrics indicate injury risks depend on impact location. Specifically, highest risks are found for impacts to the rear and side of the head, followed by the front (see Fig. 2). The injury metrics show agreement that a top impact yields the lowest risk of producing any injury to a player. Abbreviated Injury Scale 1 (AIS 1) injury risks for a passive neck condition and an inbound soccer ball velocity of 35 m/s, based on the HIC<sub>15</sub> criterion, are 18.5%, 19.3%, and 10.5% for a side, rear, and frontal impact, respectively. Additionally, AIS 2 scores, using the BrIC criterion, for the same passive neck and soccer ball velocity show 41.1%, 48.1%, 22.9%, and 1.1% injury risk probabilities for the rear, side, front, and top impacts, respectively. It should be noted that AIS head injury risks determined using CSDM-based critical values in [45] for the BrIC metric do not show a risk of a head injury. These injury risk values are expected to be representative of higher impact velocities occurring during games. The AIS injury risk scores found for a frontal impact with a passive neck condition to values of 1.5% and 0.1% using HIC<sub>15</sub> (AIS 1) and 8.6% and 1.1% using BrIC (AIS 2) for impact velocities of 23 m/s and 11 m/s, respectively. Furthermore, Fig. 2 depicts the risk of brain injury for the kinematic metrics with the highest risk of an mTBI produced by a side or rear impact (Fig. 2a). This is also correlated with the predictions of the CSDM<sub>0.05</sub> as values of 37.27% and 17.35% are predicted for the side and rear cases, respectively. All other simulations predicted a value of approximately 0% for this metric. These results also show the rear impact with the highest HIC<sub>15</sub> (180.65) and the side impact with the high BrIC (0.52) values, which indicate these impacts could pose elevated injury risks when a player is anticipating a soccer ball impact (Fig. 2b) as they produce higher AIS injury risks and associated injury concern for mTBI in soccer. Specifically, the simulation results for these impact locations are associated with over a 25% risk for mTBI based on the threshold presented in [43]. When considering the BrIC, all the simulations of the passive condition except for the top impact location indicate an AIS 2 injury risk of 22.9% – 48.1% to the head. It is noteworthy, that all these simulations are impacts along the line between the center of gravity of both the soccer ball and the head. Therefore, it can be asserted that BrIC values may be even greater if the ball were to impact off the center of the impact path due to higher rotational acceleration values.

During the passive impact condition, maximum compressive pressures at the coup site approach 150.4 kPa (side impact), and tensile pressures of -52.2 kPa (side impact) are present at the countre-coup site (Fig. 6). The highest compressive and tensile pressure values found in the side impact case correlate with the predictions of the BrIC and CSDM<sub>0.05</sub> injury metrics. For all simulation scenarios, the highest compressive pressures appear between 3 ms and 6 ms corresponding to time points near when the maximum contact area between the soccer ball and the head is achieved. The highest tensile pressures are also observed earlier in the simulation, between 3 ms and 6 ms. The peak compressive pressures throughout the brain are achieved at

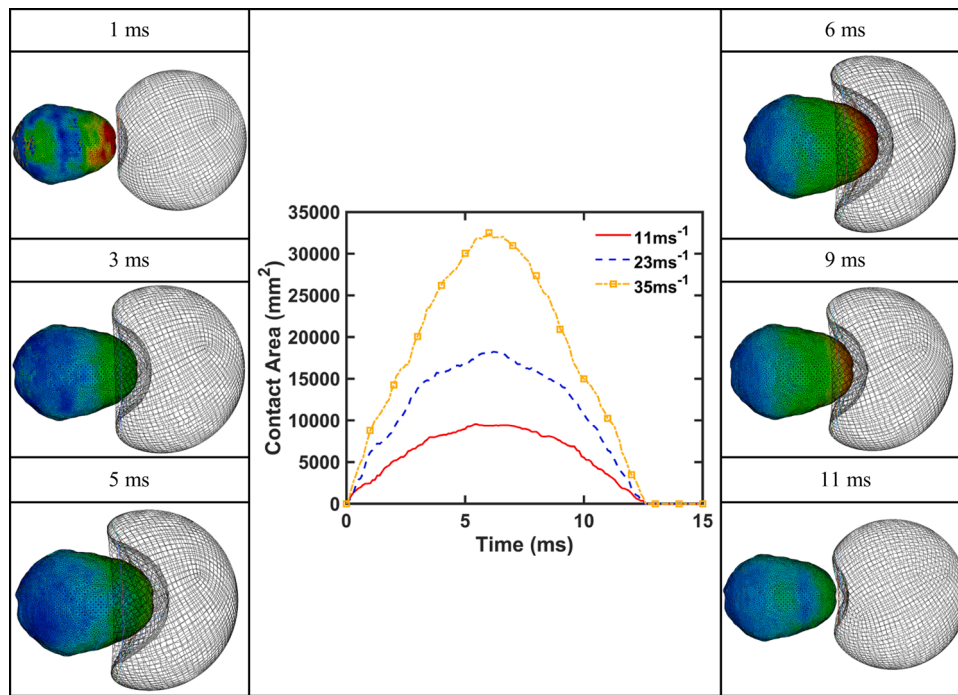


Fig. 3. Relationship between soccer ball contact area and pressure for a passive frontal heading at 35 m/s and the envelope formed by the soccer ball around the head throughout the simulation. The graph indicates the relationship between the contact area and the inbound soccer ball velocity.

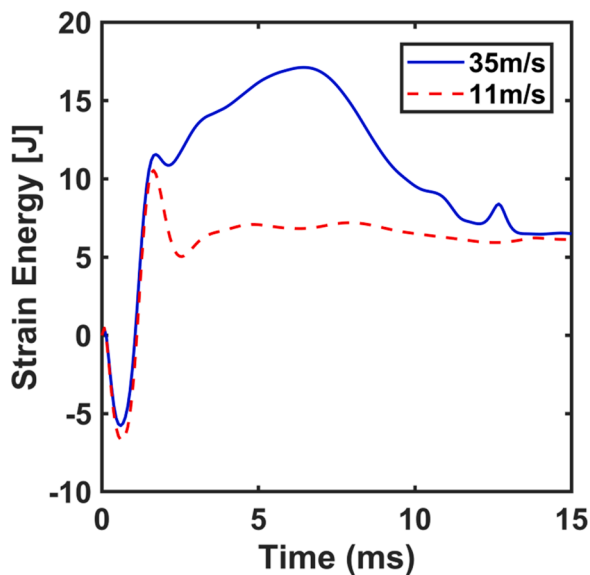


Fig. 4. Comparison of the strain energy produced by the soccer ball during a passive frontal header at impact velocities of 11 m/s and 35 m/s.

approximately 6 ms, after which the tensile pressures in the countercoup site begin to decline (Fig. 6). These tensile pressures continue to decline as the ball rebounds from the head (between 6 ms and 12 ms) until predominantly compressive pressures are seen at the countercoup site during the final segment of the impact at approximately 12 ms (Fig. 6).

The most common on-field impact location is the forehead region. A rear impact would be less likely due to a soccer player’s preferentially heading a soccer ball at the forehead. This preferential forehead heading may underrepresent the number of incidences resulting from the rear impact mTBI. The ball contacting the top vertices of the head indicates the least likelihood of injury risk. A vertex impact would limit the

possible head movement due to the rest of the body providing additional stiffness. This type of location dependency of injury risk has also been shown in American football impacts, as those occurring to the top or front of the helmet produced lower strains than those observed at other locations [46].

Additionally, an increase in the inbound soccer ball velocities shows a correspondingly increased injurious risk, according to the HIC<sub>15</sub> and BrIC injury metrics (Fig. 2c, d). The AIS 1 injury risks, due to an increase in the inbound ball velocity from 11 m/s to 35 m/s, increase the HIC<sub>15</sub> injury metric from 0.1% to 10.5%, and the AIS 2 injury risks increase for BrIC from 1.1% to 22.9%. These increased values are not surprising, given the increase in kinetic energy at the highest soccer ball velocities; however, it is a noteworthy aspect of the injury mechanisms of a soccer heading.

#### 4.2. Active versus passive neck heading

There are substantial differences between the severity of the risk of brain injury resulting from the active and passive ball-head impact conditions. When comparing the active and passive cases, the pressure profile changes at the larger, increased time scales (Figs. 5, and 6), where head displacement is apparent. When the neck muscles are not active, a passive neck is stimulated. During this case, for a frontal ball-head impact, the backward head motion creates a coup-countercoup pressure profile (Fig. 5 passive and Fig. 6), with positive magnitudes of pressure in the frontal lobe and negative pressures in the occipital lobe and the cerebellum. Similar pressure profiles are also seen for lateral and rear ball-head impact cases when the neck is relaxed (Fig. 6c, d) with either tensile or extremely low compressive pressures at the countercoup location. In comparison, when the soccer player is aware of the ball, with active neck muscle engagement and lack of head movement, the coup-countercoup mechanism is still observed through 9 ms (Fig. 5 Active Condition); however, compressive pressures are observed at the countercoup site later in the simulation (12 ms), and the pressure magnitudes at both coup (compressive pressures) and countercoup (tensile pressures) are lower than the passive cases throughout the entire duration of the impact (Fig. 5 Passive Condition).

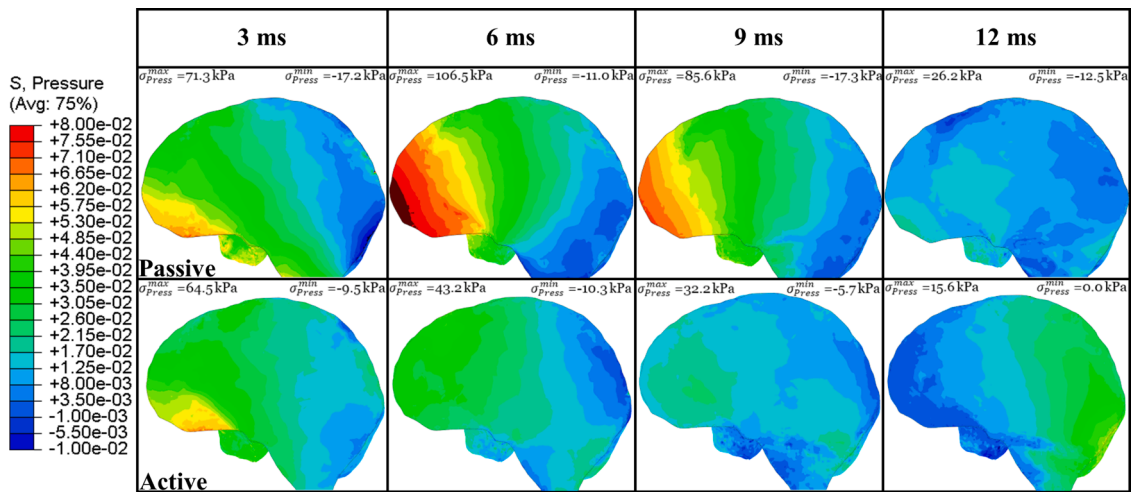


Fig. 5. Passive vs active pressure (MPa) propagation for a frontal soccer ball heading at 35 m/s.  $\sigma_{Press}^{min}$  is the maximum tensile pressure and  $\sigma_{Press}^{max}$  is the maximum compressive pressure measured at the ccontre-coup and coup sites respectively.

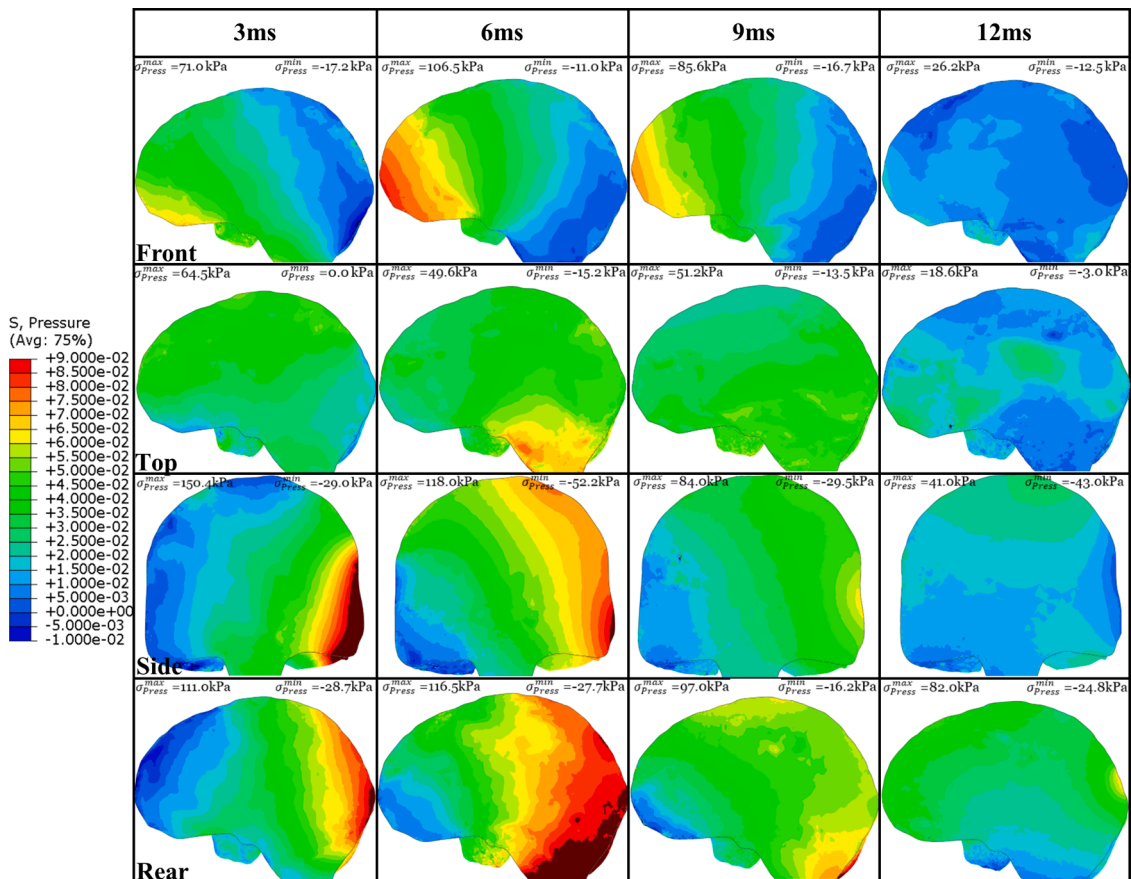


Fig. 6. Pressure (MPa) propagation for passive soccer ball heading at various locations at 35 m/s.  $\sigma_{Press}^{min}$  is the maximum tensile pressure and  $\sigma_{Press}^{max}$  is the maximum compressive pressure measured at the ccontre-coup and coup sites respectively.

The passive condition represents a player who is not anticipating contact with the ball, such that the head is displaced without active musculoskeletal restraint and produces more significant linear and rotational accelerations and poses a greater risk of injury. A passive ball-to-head contact type is considered to be an increased risk for elevated brain injuries in soccer [47]. Similar trends of heightened stress and strain states for passive neck heading are observed regionally near the impact site and throughout the full brain. Interestingly, elevated stresses

and strains are observed in brain regions opposite the impact site in the active condition as compared to the passive condition; however, peak values for the full brain show reduced values for the pressure and max principal strain values in the passive case for all impact locations. This is illustrated by average pressure, Von Mises stress, and maximum principal strain peak values presented in Table 2. The increase of head injury caused by passive neck heading is further demonstrated in the wider range and increased severity of pressure values in the contour plots of

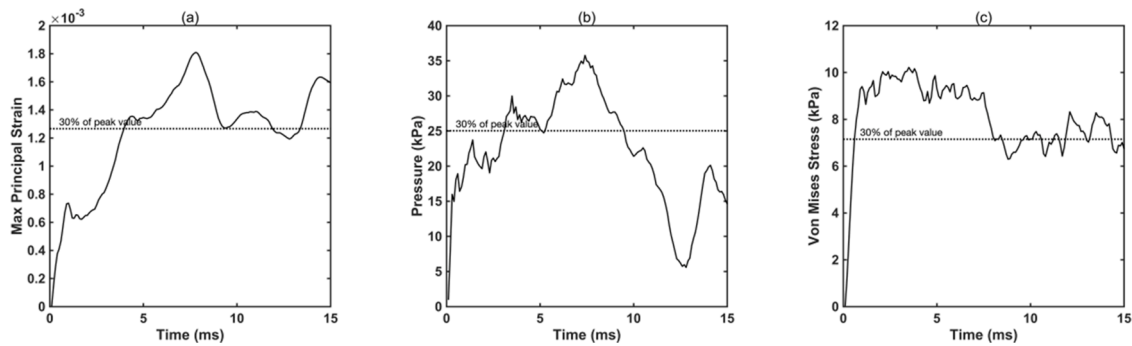


Fig. 7. Time histories for the maximum principal strain (a), pressure (b), and Von Mises stress (c) responses for the full brain of a passive frontal impact at 35 m/s.

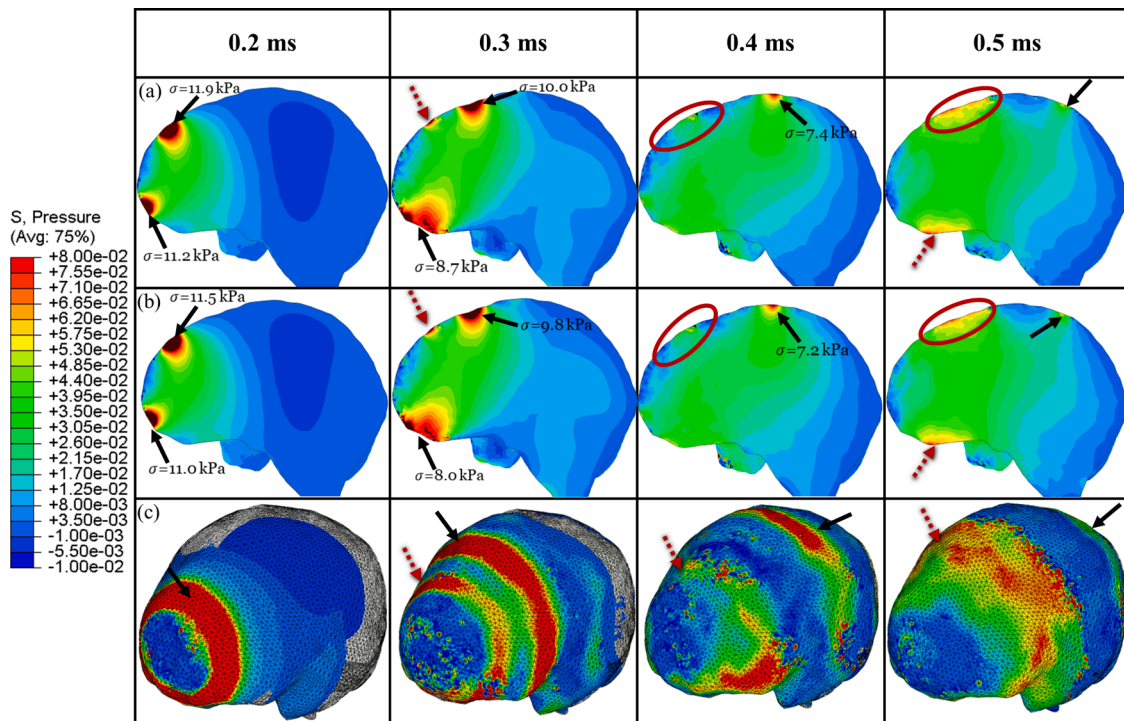


Fig. 8. Initial pressure (MPa) propagation throughout the FE brain for a passive (a) and active (b) frontal header at 35 m/s with the peak values of pressure shown for the initial stress wave in both neck conditions. The pressure propagation around the brain for the passive impact case is presented in (c) to exemplify the “ring shaped” pressure waves. The black arrows show the cross section of the first pressure wave and the red (arrow and circled) show the second pressure wave.

Fig. 5. Furthermore, the magnitude of the initial pressure waves propagating through the cerebral cortex are elevated, due to the decreased neck stiffness (Fig. 8a, b).

The active condition is controlled movement of the forehead towards the ball with an associated bracing of the neck muscles to resist recoil as the ball impacts the head. As the neck musculature stiffens up as one is anticipating the incoming ball, the head being “connected” to the body produces significantly lower magnitudes of transitional and rotational head displacement. All AIS injury risks are reduced considerably when the neck constraint is active and indicates injury risk reductions to values under approximately 1% (front, side, top impact locations) or 5.8% (rear impact case) for the HIC<sub>15</sub> metric (AIS 1) and under approximately 2% for the BrIC (AIS 2) criteria (Fig. 2a). Additionally, the CSDM<sub>0.05</sub> metric showed values of approximately 0% for all impact locations in the active condition. Brain injuries are due to excessive linear and rotational head accelerations that cause deformation [48]. Anticipation is also associated with a reduction in injury severity during collisions between players in ice hockey [49]. The reduced BrIC and HIC15 values evidence this concept (Fig. 2b). Additionally, on-field

studies of soccer headers have indicated as the neck muscles are increasingly activated, the head accelerations and the forces produced on the head are reduced [50]. Previous researchers have demonstrated this correlation between head acceleration and brain injuries in experimental rodent studies [51]. The immobilization of a mouse’s head showed reduced learning ability and memory defects [51].

#### 4.3. Brain injury metrics comparison

Fig. 2 and Table 2 provide the associated BrIC, HIC<sub>15</sub>, peak pressure, Von Mises stress, and max principal strain values produced within the regions of the brain and entire brain for soccer ball impacts at 35 m/s to the front, lateral, top, and rear of an athlete’s head. These impact metrics’ results are for both active and passive neck bracing. Rear and side impacts notably produce the highest values in terms of HIC<sub>15</sub>, and BrIC injury risks, which correlates with the highest peak pressure at 99.5 kPa corresponding to the cerebellum region of the brain during a rear soccer header in the passive case and the highest maximum principal strain of 0.0573 in the cerebellum region during a side impact header in the



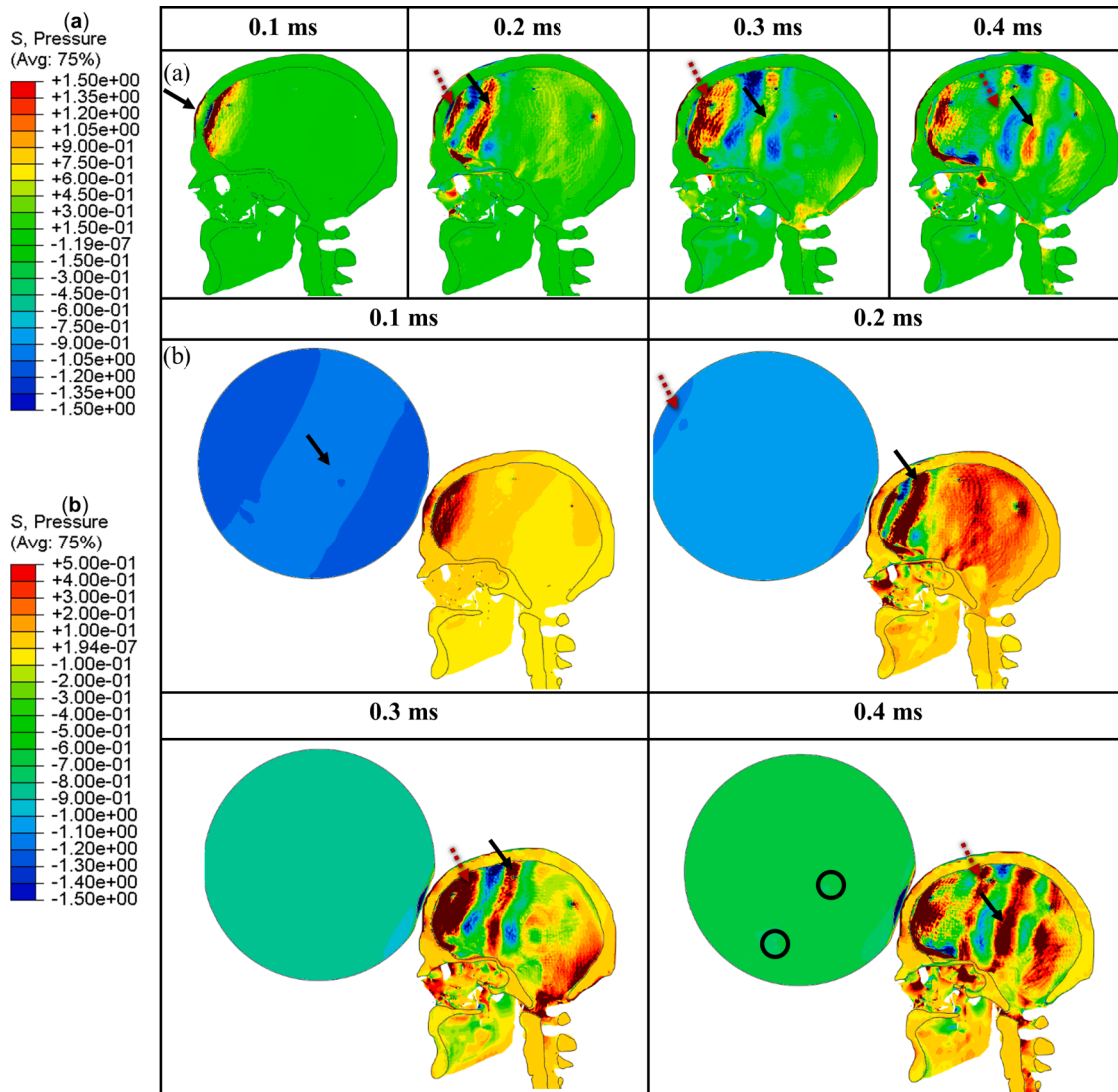


**Fig. 9.** Initial pressure (MPa) propagation of the stress wave through the skull (scalp and brain removed) (a) and the transfer of the stress wave from the soccer ball to the head (scalp and brain removed) (b). The black arrows indicate the first stress wave transferred from the ball to the skull and red arrows indicate the second stress wave. Other indications of stress transfer between the ball and skull are marked by the black circle.

passive neck condition (Fig. 2a, b, and Table 2). The HIC<sub>15</sub> predicted that the side and rear impacts are the most likely to produce an injury in passive neck conditions, whilst the rear impact has the highest risk of injury in the active neck conditions (Fig. 2a). The BrIC predicted the side and rear impacts have the highest risk of injury in the passive and active neck condition (Fig. 2b). Furthermore, the kinematic injury predictors also indicate a risk of higher injury severity at greater inbound soccer ball velocities. The peak values of pressure and maximum principal strain also indicate increased magnitudes during the side and rear impacts (Table 2). The pressure values that correspond to the peak values are almost exclusively determined at the time of maximum contact between the soccer ball and the head. This trend is most clearly observed for the brain lobes nearest to the impact site. Brain lobes opposite to the location of impact show reduced pressure values, with the peak response values still corresponding to the maximum contact area or during a relatively constant response. Von Mises stress values reach their maximum before the peak contact area occurred (at approximately 3 ms). The maximum principal strain values showed a more constant trend, with peak values occurring after the maximum contact area is achieved (around 10 ms). The influence of anticipation of incoming soccer ball impacts indicates a significant reduction in peak values when comparing the passive and active neck conditions (Fig. 2a, b).

Interestingly, the side impact produces elevated values in the pressure variable in the active neck response conditions, based on the peak values shown in Table 2. Also, lower magnitude values are predicted in the top impact case for both the passive and active cases in the considered kinematic variables (Fig. 2a,b).

Brain injury indicators are a widely studied topic, due to the complexities of understanding and predicting injuries. Additionally, comprehending and diagnosing brain injuries caused by soccer ball heading is especially challenging. Until recently, any potential brain injury occurring during a soccer game has been expected to produce milder symptoms, which may not be diagnosed as a TBI. This correlates with the minimally reported concussions sustained from head-to-ball contact [52]. The risk assessment for soccer ball headings is important for understanding how to improve the safety of this sport and develop countermeasures that promote the safety of athletes. The results of the present simulations indicate there is a risk of mTBI when heading a soccer ball, most significantly during the rear and side-impact scenarios (Fig. 2). However, the potential injury severity of any impact is challenging to distinguish and define, particularly for sub-concussive and concussive injuries, due to a lack of corresponding clinically observed data for the creation of injury thresholds and risk curves. A better understanding of these types of injury metrics when studying sports-related

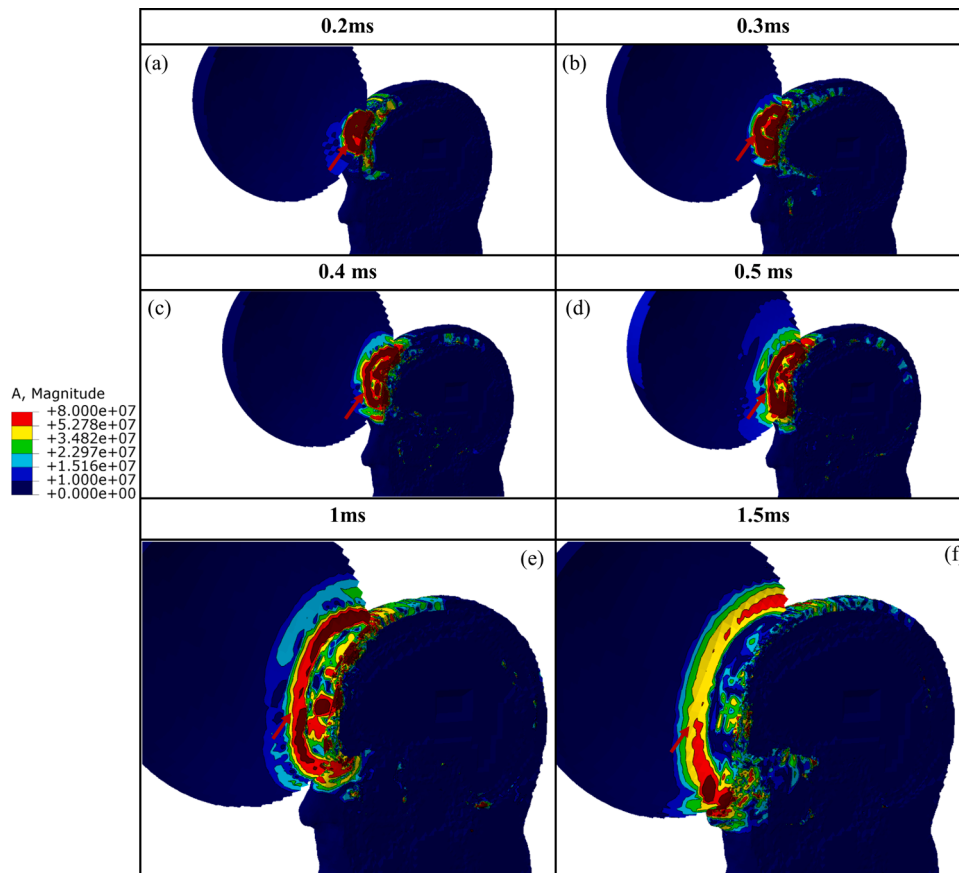


**Fig. 10.** Contour plot showing the magnitude of the acceleration ( $\text{mm/s}^2$ ) for the contact interface of the soccer ball and human head using a logarithmic scale to show the peak resultant accelerations to be found at the edges of the contact surface between the soccer ball and the head at times 0.2 ms, 0.3 ms, 0.4 ms 0.5 ms, (a,b, c,d) 1ms, and 1.5 ms (e,f). The red arrows denote the peak accelerations on the soccer ball forming the “ring shaped” pattern on the contact interface.

mTBIs is needed. The greatest danger to the head health of soccer players may not be the single, acute exposures associated with head-on-head or head-on-surface contacts, but the cumulative effects of repeated sub-clinical exposures associated with soccer ball headings. An improved injury metric that includes representations of sub-concussive and concussive impacts would significantly improve the understanding of sports-related mTBI. Particular emphasis should be placed on understanding the relationship between the duration of brain exposure at impact energy level (over a period of time) and the associated risk of injury. Most injury metrics correlate maximum values of their respective criterion to determine the risk of injury, not the peak exposure duration. Injury metrics that include time-dependent considerations of these metrics could be considered to define better the risk of head-to-ball contact TBI in soccer and other related sports injuries.

#### 4.4. Stress wave propagation

Since a soccer ball is pressurized, tensile and compressive stress waves are produced in the ball during a heading impact. These tensile and compressive stress waves correspond to the tensile and compressive pressure evolution, respectively. At the onset of the ball-head impact, the tensile pressures are transformed into compressive pressure as the ball deforms and wraps around the head contact surface, which is produced at the ball's point of impact and then transferred into the head of the athlete (Figs. 3 and 9). As the initial contact occurs, these tensile pressures can be seen (Fig 9b; black arrow) at 0.1 ms in the soccer ball. As the impact continues, the initial stress waves are transmitted to the scalp and skull as the peak compressive pressures, shown in the 0.2ms time step. During this time, the emergence of a second tensile stress

wave is seen at the rear side of the soccer ball, as the pressures are continuously transmitted through the ball (red arrow) and then into the scalp and skull, in the 0.3 ms time step. Simultaneously, as the wavefront traverses through the skull, it also transmits into the brain tissue, creating a ring-shaped, circular pressure profile, the cross-section of which is shown with black arrows at locations adjacent to the wavefront in the skull, as seen by the high magnitudes in Fig. 8, at 0.2, 0.3, 0.4, and 0.5 ms. Here, it is to be noted that the longitudinal stress waves move significantly faster in the skull than in the brain tissue, mainly due to the stiffness difference between the skull and the brain tissue. Hence, the stress waves travel faster in the skull than in the brain. The ring-shaped stress waves can be seen to travel around the brain, see Fig. 8c, and are caused most notably by the high tensile pressures in the ball being located at the center point of the contact area, which create a “cup-like” region in the contact surface (Fig. 3). Surrounding this high tensile region are the ball's highest compressive pressures, which mark the initiation point for the stress wave transmission from the soccer ball to the head during this contact. The ring-shaped pattern of the stress waves can be further illustrated by the corresponding high accelerations found at the edges of the contact surface in the soccer ball and the scalp (Fig. 10). As the impact progresses, these peak accelerations are seen to expand radially along with the edge of the contact surface to form the circular shapes found in the stress waves transmitted from the soccer ball to the brain presented in Fig. 8. The magnitude of the stress wave then decreases as it travels through the scalp, skull, and CSF and damps out to lower values due to the poroviscous nature of the soft tissue in the head [53,54]. At 0.3 ms, a new peak pressure (red arrow) is introduced to a second stress wavefront (Fig. 8). The location of the high magnitude ring-shaped pressure profile within the cerebral cortex is of some

concern, since they have been shown to generate shear stresses at the sulcus base, the location of which correlates with CTE [55–57]. This would correspond with the findings of other authors, who have suggested a correlation between repetitive soccer headers and CTE in post-mortem human subjects [58]. Furthermore, the behavior of the stress wave is shown to traverse through the thickness of the skull, in conjunction with the stress waves seen in the brain. These waves are found to extend across a greater surface area and are of a much higher magnitude than those in the brain, with peak compressive pressure values exceeding 1.5 MPa.

#### 4.5. Dynamics of soccer ball-head contact area

A significant difference between soccer ball impacts and those associated with firmer, unyielding surfaces is the relatively longer contact durations. The pliancy of the ball results in a longer (12 ms) and more delayed energy transfer. Fig. 7 shows that peak stresses and strains in the brain reach a plateau, after a sharp initial increase, due to the transfer of energy from the ball deformation to the head and then to the brain. The transfer of energy occurs over a large contact surface area, with the duration of the energy transfer independent of the impact velocity (Fig. 3). A relatively large contact surface area and a delayed energy transfer are associated with a reduced risk of skull fracture and skull fracture-related brain injury compared with a low contact area and high magnitude forces. However, a significant amount of energy is still transferred into the head and the brain with a passive frontal impact of 35 m/s transferring approximately 100 J into the head. Additionally, the peak energy transfer occurs at the peak contact area for this impact scenario (Fig. 4). Notably, a strong difference is observed between the energy transfer at the higher and lower impact velocities with an 11 m/s passive frontal impact indicating a transfer of 10 J to the head and the strain energy indicating a decrease in energy after the initiation of contact (Fig. 4). While concussions, due to ball-headings, are not as common as other contact sports (such as football or hockey [59–61]), the risk of sub-concussive injury in headings is suspected to be high, with clinical studies suggesting the adverse effects of headings on cognitive impairment [62]. Specifically, there is a lack of documented concussive diagnosis resulting from soccer headers; however, studies have correlated neurological deficits due to headings [63] indicating the potential of injury below concussive levels.

#### 4.6. Limitations and future work

The FE head model used throughout this effort is a 50th percentile male head model used in a prior study [31]. This model does not account for other head anthropometric differences present for different athletes throughout the sport. Conclusions as to the degree and probability of injuries in soccer are somewhat limited in this study, due to a lack of consensus among the current injury metrics and the limited studies of clinical observations of brain injuries in soccer. Additionally, this study did not consider a female FE head model, limiting the inferences that could be applied to women's soccer-related TBI. Female athlete headers warrant future studies with respect to any potential differences between female and male header participants. Further, the FE head model does not include a validated incorporation of the human neck and corresponding muscles. Future work will include the development and implementation of a further developed and validated cervical neck FE model. This FE model will enable future research to explore more extensively the role of the activation of the muscular network throughout the neck and its contribution to reducing injury risks associated with soccer headings. This study also lacks a characterization of the uncertainty due to the experimental studies and computational simulations. Additionally, future work will have to include a sensitivity analysis for these results to better understand the robustness of the simulation results, due to the input parameter changes in the FE head model. Furthermore, different soccer ball inflation pressures have been

shown to affect the behavior of the soccer ball and the response of the athlete's head [64–66]. Future work will also include finite element simulations, which evaluate the head response for different soccer ball inflation pressures to provide additional insight into these sensitivities and injury risks associated with different inflation pressures.

## 5. Conclusion

The brain injury risk of soccer ball headings has not been well understood or defined. The simulations evaluate the effect of soccer ball impact velocity, impact location and the effects of anticipation of an incoming soccer ball. The simulations show increasing soccer ball velocities and an impact to the side and rear, followed by the front of the head, pose the greatest risk of injury (Fig. 2a–d, Table 2, Fig 6). The lack of anticipation of an incoming soccer ball by an athlete, referred to as a passive heading in this study, produces a much greater injury risk than a typical soccer ball heading when the athlete's neck musculoskeletal features are activated (Table 2, Figs. 2a, b and 5). Additionally, the simulations show that the pressure waves within the soccer ball are transferred to the head upon impact and propagate throughout the scalp, skull, CSF and the brain (Figs. 8, 9). Furthermore, these pressure waves manifest as compressive and tensile waves in the cerebral cortex of the brain (Figs. 5, 6, 8). Also, the soccer ball's contact surface is unique when impacting the head and strongly influences the resulting stress waves and their severity on the brain (Figs. 3, 4). This contact surface causes an extended duration of energy transfer in comparison to other sports-related head trauma mechanisms (Fig. 7). Moreover, the shape of the stress waves is heavily influenced by this contact interaction (Fig. 10). The results of this study give insight into the potential risk of headers in soccer and possible methods to improve the safety of an athlete. Lastly, brain injury metrics indicate discrepancies in the degree of injury risks for the soccer headers and emphasized the importance of developing new injury metrics to better predict sub concussive, concussive, and mTBI injuries in sports (Fig. 2).

### Statement of significance

Mild traumatic brain injuries (mTBI) are a worrisome aspect of participation in most sports due to difficulties in their diagnosis in competitions and the potential of long-term neurological defects. These types of injuries are not well understood for athletes playing soccer, specifically pertaining to the risks of heading a soccer ball. Studies are warranted which investigate impacts in this game to improve current knowledge. Our computational study uses finite element modeling to investigate contact between a player's head and the soccer ball. The results of this study present potential injury mechanisms and risks caused by this contact interaction to contribute to the current understanding of brain injuries in soccer and the promotion of athlete safety.

### Ethical statement

No human or animal experiments were performed in this study.

### Declaration of Competing Interest

The authors declare that they have no known competing financial interests or personal relationships that could have appeared to influence the work reported in this paper.

### Acknowledgments

The authors would like to acknowledge the Center for Advanced Vehicular Systems (CAVS) at Mississippi State University for supporting this work.

## Supplementary materials

Supplementary material associated with this article can be found, in the online version, at [doi:10.1016/j.brain.2022.100052](https://doi.org/10.1016/j.brain.2022.100052).

## References

- [1] V. Hubertus, N. Marklund, P. Vajkoczy, Management of concussion in soccer, *Acta Neurochir.* 161 (3) (2019) 425–433, <https://doi.org/10.1007/s00701-019-03807-6>. Mar.
- [2] D. Deprez, J. Fransen, J. Boone, M. Lenoir, R. Philippaerts, R. Vaeyens, Characteristics of high-level youth soccer players: variation by playing position, *J. Sports Sci.* 33 (3) (2015) 243–254, <https://doi.org/10.1080/02640414.2014.934707>. Feb.
- [3] L.M. Quintero, et al., Reducing risk of head injury in youth soccer: an extension of behavioral skills training for heading, *J. Appl. Behav. Anal.* (2019). Mar. 29, <https://onlinelibrary.wiley.com/doi/abs/10.1002/jaba.557>. accessed Jun. 19, 2019.
- [4] R.S. Naunheim, J. Standeven, C. Richter, L.M. Lewis, Comparison of impact data in hockey, football, and soccer, *J. Trauma Acute Care Surg.* 48 (5) (2000) 938–941. May.
- [5] M.E. Maher, M. Hutchison, M. Cusimano, P. Comper, T.A. Schweizer, Concussions and heading in soccer: a review of the evidence of incidence, mechanisms, biomarkers and neurocognitive outcomes, *Brain Inj.* 28 (3) (2014) 271–285, <https://doi.org/10.3109/02699052.2013.865269>. Mar.
- [6] R. Dick, M. Putukian, J. Agel, T.A. Evans, S.W. Marshall, Descriptive epidemiology of collegiate women's soccer injuries: national collegiate athletic association injury surveillance system, 1988–1989 Through 2002–2003, *J. Athl. Train.* 42 (2) (2007) 278–285.
- [7] M.L. Levy, A.S. Kasasbeh, L.C. Baird, C. Amene, J. Skeen, L. Marshall, Concussions in soccer: a current understanding, *World Neurosurg.* 78 (5) (2012) 535–544, <https://doi.org/10.1016/j.wneu.2011.10.032>. Nov.
- [8] J.S. Delaney, V.J. Lacroix, S. Leclerc, K.M. Johnston, Concussions among university football and soccer players, *Clin. J. Sport Med.* 12 (6) (2002) 331–338. Nov.
- [9] T. Bey, B. Ostick, Second impact syndrome, *West J. Emerg. Med.* 10 (1) (2009) 6–10. Feb.
- [10] A.C. McKee, et al., The spectrum of disease in chronic traumatic encephalopathy, *Brain* 136 (1) (2013) 43–64, <https://doi.org/10.1093/brain/aww307>. Jan.
- [11] C.M. Baugh, et al., Chronic traumatic encephalopathy: neurodegeneration following repetitive concussive and subconcussive brain trauma, *Brain Imaging Behav.* 6 (2) (2012) 244–254, <https://doi.org/10.1007/s11682-012-9164-5>. Jun.
- [12] E.J.T. Matser, A.G. Kessels, M.D. Lezak, B.D. Jordan, J. Troost, Neuropsychological impairment in amateur soccer players, *JAMA* 282 (10) (1999) 971–973, <https://doi.org/10.1001/jama.282.10.971>. Sep.
- [13] M.H.A. Hassan, Z. Taha, Finite element analysis of soccer heading, *Proc. Eng.* 112 (2015) 46–51, <https://doi.org/10.1016/j.proeng.2015.07.174>.
- [14] Z. Taha, M.H.A. Hassan, A reaction-force-validated soccer ball finite element model, *Proc. IMechE* 231 (1) (2017) 43–49, <https://doi.org/10.1177/1754337115626636>. Mar.
- [15] P.Y. Chen, L.S. Chou, C.J. Hu, H.H. Chen, Finite element simulations of brain responses to soccer-heading impacts. 1st Global Conference on Biomedical Engineering & 9th Asian-Pacific Conference on Medical and Biological Engineering, Cham, 2015, pp. 118–119, [https://doi.org/10.1007/978-3-319-12262-5\\_33](https://doi.org/10.1007/978-3-319-12262-5_33).
- [16] M.L. Levy, A.S. Kasasbeh, L.C. Baird, C. Amene, J. Skeen, L. Marshall, Concussions in soccer: a current understanding, *World Neurosurg.* 78 (5) (2012) 535–544, <https://doi.org/10.1016/j.wneu.2011.10.032>. Nov.
- [17] J.T. Matser, A.G.H. Kessels, M.D. Lezak, J. Troost, A dose-response relation of headers and concussions with cognitive impairment in professional soccer players, *J. Clin. Exp. Neuropsychol.* 23 (6) (2001) 770–774, <https://doi.org/10.1076/jcen.23.6.770.1029>. Dec.
- [18] C. Withnall, Effectiveness of headgear in football, *Br. J. Sports Med.* 39 (2005) i40–i48, <https://doi.org/10.1136/bjism.2005.019174>. Supplement 1Aug.
- [19] V.C. Prabhu, J.E. Baines, Chronic subdural hematoma complicating arachnoid cyst secondary to soccer-related head injury: case report, *Neurosurgery* 50 (1) (2002) 195–198, <https://doi.org/10.1097/00006123-200201000-00029>. Jan.
- [20] B.D. Stemper, F.A. Pintar, Biomechanics of concussion, *Concussion* 28 (2014) 14–27, <https://doi.org/10.1159/000358748>.
- [21] T.W. Kaminski, A. Thompson, V.E. Wahlquist, J. Glutting, Self-reported head injury symptoms exacerbated in those with previous concussions following an acute bout of purposeful soccer heading, *Res. Sports Med.* 28 (2) (2020) 217–230, <https://doi.org/10.1080/15438627.2019.1635130>. Apr.
- [22] A. Al-Kashmiri, J.S. Delaney, Head and neck injuries in football (soccer, trauma. 8 (3) (2006) 189–195, <https://doi.org/10.1177/1460408606071144>. Jul.
- [23] J.A. Bauer, T.S. Thomas, J.H. Cauraugh, T.W. Kaminski, C.J. Hass, Impact forces and neck muscle activity in heading by collegiate female soccer players, *J. Sports Sci.* 19 (3) (2001) 171–179, <https://doi.org/10.1080/026404101750095312>. Jan.
- [24] G.M. Gutierrez, C. Conte, K. Lightbourne, The relationship between impact force, neck strength, and neurocognitive performance in soccer heading in adolescent females, *Pediatr. Exerc. Sci.* 26 (1) (2014) 33–40, <https://doi.org/10.1123/pes.2013-0102>. Feb.
- [25] Z.D.W. Dezman, E.H. Ledet, H.A. Kerr, Neck strength imbalance correlates with increased head acceleration in soccer heading, *Sports Health* 5 (4) (2013) 320–326, <https://doi.org/10.1177/1941738113480935>. Jul.
- [26] C. Kuo, J. Sheffels, M. Fanton, I.B. Yu, R. Hamalainen, D. Camarillo, Passive cervical spine ligaments provide stability during head impacts, *J. R. Soc. Interface.* 16 (154) (2019), 20190086, <https://doi.org/10.1098/rsif.2019.0086>. May.
- [27] D.S. Price, R. Jones, A.R. Harland, Computational modelling of manually stitched soccer balls, *Proc. IMechE* 220 (4) (2006) 259–268, <https://doi.org/10.1243/14644207JMDA83>. Oct.
- [28] FIFA, “Laws of the game 2021/2022,” 2021.
- [29] R. Prabhu, et al., Coupled experiment/finite element analysis on the mechanical response of porcine brain under high strain rates, *J. Mech. Behav. Biomed. Mater.* 4 (7) (2011) 1067–1080, <https://doi.org/10.1016/j.jmbbm.2011.03.015>. Oct.
- [30] R. Prabhu, et al., A coupled experiment-finite element modeling methodology for assessing high strain rate mechanical response of soft biomaterials, *JoVE* (99) (2015) 51545, <https://doi.org/10.3791/51545>. May.
- [31] K.L. Johnson, et al., Constrained topological optimization of a football helmet facemask based on brain response, *Mater. Des.* 111 (Dec. 2016) 108–118, <https://doi.org/10.1016/j.matdes.2016.08.064>.
- [32] A. M. Nahum, R. Smith, and C. C. Ward, “Intracranial pressure dynamics during head impact,” Feb. 1977, p. 770922. doi: 10.4271/770922.
- [33] W.N. Hardy, C.D. Foster, M.J. Mason, K.H. Yang, A.I. King, S. Tashman, Investigation of head injury mechanisms using neutral density technology and high-speed biplanar X-ray, *Stapp Car Crash J.* 45 (Nov. 2001) 337–368.
- [34] A.V. Tran, Q.H. Hoang, A.T. Nguyen, V.T. Le, V.K. Le, T.V.H. Pham, The models of relationship between center of gravity of human and weight, height and 3 body's indicators (Chest, waist and hip), *J. Sci. Technol. Univ.* 139 (2019). Accessed: Sep. 20, 2020. [Online]. Available, <https://eprints.uet.vnu.edu.vn/eprints/doi/epri/nt/3913/>.
- [35] M. Damavandi, P. Allard, F. Barbier, J. Leboucher, C. Rivard, and N. Farahpour, “Estimation of whole body moment of inertia using self-imposed oscillations,” 2006. <https://www.semanticscholar.org/paper/Estimation-of-Whole-Body-Moment-of-Inertia-Using-Damavandi-Allard/edf32ba11338015c1af1346518371ba5e897105b> (accessed Jun. 11, 2022).
- [36] A. Trotta, J.M. Clark, A. McGoldrick, M.D. Gilchrist, A.N. Annaidh, Biofidelic finite element modelling of brain trauma: importance of the scalp in simulating head impact, *Int. J. Mech. Sci.* 173 (2020), 105448, <https://doi.org/10.1016/j.ijmecsci.2020.105448>. May.
- [37] M. Tomáš, Z. František, M. Lucia, T. Jaroslav, Profile, correlation and structure of speed in youth elite soccer players, *J. Hum. Kinet.* 40 (2014) 149–159, <https://doi.org/10.2478/hukin-2014-0017>. Apr.
- [38] H. Nunome, Y. Ikegami, R. Kozakai, T. Apriantono, S. Sano, Segmental dynamics of soccer instep kicking with the preferred and non-preferred leg, *J. Sports Sci.* 24 (5) (2006) 529–541, <https://doi.org/10.1080/02640410500298024>. May.
- [39] T. Asami, V. Nolte, H. Matsui, K. Kobayashi, *Biomechanics VIII-B*, Hum. Kinet. Champaign, IL (1983).
- [40] A. Radja, M. Erceg, Z. Grgantov, Inter and intra positional differences in ball kicking between U-16 Croatian soccer players, *Montenegrin J. Sports Sci. Med.* 5 (2) (2016) 11.
- [41] L. Miller, J. Gaewsky, A. Weaver, J. Stitzel, and N. White, “Regional level crash induced injury metrics implemented within THUMS v4.01,” Apr. 2016, pp. 2016-01–1489. doi: 10.4271/2016-01-1489.
- [42] E. G. Takhounts, M. J. Craig, K. Moorhouse, J. McFadden, and V. Hasija, “Development of brain injury criteria (BrIC),” Nov. 2013, pp. 2013-22–0010. doi: 10.4271/2013-22-0010.
- [43] L. Zhang, K.H. Yang, A.I. King, A proposed injury threshold for mild traumatic brain injury, *J. Biomech. Eng.* 126 (2) (2004) 226–236, <https://doi.org/10.1115/1.1691446>. May.
- [44] A.A. Weaver, K.A. Danelson, J.D. Stitzel, Modeling brain injury response for rotational velocities of varying directions and magnitudes, *Ann. Biomed. Eng.* 40 (9) (Sep. 2012) 2005–2018, <https://doi.org/10.1007/s10439-012-0553-0>.
- [45] E. G. Takhounts, M. J. Craig, K. Moorhouse, J. McFadden, and V. Hasija, “Development of brain injury criteria (BrIC),” Nov. 2013, pp. 2013-22–0010. doi: 10.4271/2013-22-0010.
- [46] B.S. Elkin, L.F. Gabler, M.B. Panzer, G.P. Siegmund, Brain tissue strains vary with head impact location: a possible explanation for increased concussion risk in struck versus striking football players, *Clin. Biomech.* 64 (2019) 49–57, <https://doi.org/10.1016/j.clinbiomech.2018.03.021>. Apr.
- [47] D.T. Kirkendall, S.E. Jordan, W.E. Garrett, Heading and head injuries in soccer, *Sports Med.* 31 (5) (2001) 369–386, <https://doi.org/10.2165/00007256-200131050-00006>. Apr.
- [48] S. Signoretto, G. Lazzarino, B. Tavazzi, R. Vagnozzi, The pathophysiology of concussion, *PM&R* 3 (10) (2011) S359–S368, <https://doi.org/10.1016/j.pmrj.2011.07.018>. Supplement 2Oct.
- [49] J.P. Mihalik, J.T. Blackburn, R.M. Greenwald, R.C. Cantu, S.W. Marshall, K. M. Guskiewicz, Collision type and player anticipation affect head impact severity among youth ice hockey players, *Pediatrics* 125 (6) (2010) e1394–e1401, <https://doi.org/10.1542/peds.2009-2849>. Jun.
- [50] M.T.O. Worsey, B.S. Jones, A. Cervantes, S.P. Chauvet, D.V. Thiel, H.G. Espinosa, Assessment of head impacts and muscle activity in soccer using a t3 inertial sensor and a portable electromyography (EMG) system: a preliminary study, *Electronics* 9 (5) (2020), <https://doi.org/10.3390/electronics9050834>. Art5May.
- [51] L. Goldstein, et al., Chronic traumatic encephalopathy in blast-exposed military veterans and a blast neurotrauma mouse model, *Sci. Transl. Med.* (2012), <https://doi.org/10.1126/scitranslmed.3003716>.
- [52] M.W. Niedfeldt, Head injuries, heading, and the use of headgear in soccer, *Curr. Sports Med. Rep.* 10 (6) (2011) 324–329, <https://doi.org/10.1249/JSR.0b013e318237be53>. Dec.

- [53] A.D. Brown, K.A. Rafaels, T. Weerasooriya, Microstructural and Rate-Dependent Shear Response of Human Skull Bones, CCDC Army Research Laboratory Aberdeen Proving Ground, United States, 2020. MarAccessed: Oct. 26, 2021. [Online]. Available, <https://apps.dtic.mil/sti/citations/AD1093618>.
- [54] G. McIlvain, H. Schwarb, N.J. Cohen, E.H. Telzer, C.L. Johnson, Mechanical properties of the in vivo adolescent human brain, *Dev. Cogn. Neurosci.* 34 (Nov. 2018) 27–33, <https://doi.org/10.1016/j.dcn.2018.06.001>.
- [55] A. Bakhtiarydavijani, et al., A mesoscale finite element modeling approach for understanding brain morphology and material heterogeneity effects in chronic traumatic encephalopathy, *Comput. Meth. Biomech. Biomed. Eng.* 0 (0) (2021) 1–15, <https://doi.org/10.1080/10255842.2020.1867851>. Feb.
- [56] B.T. Fagan, S.S. Satapathy, J.N. Rutledge, S.E. Kornguth, Simulation of the strain amplification in sulci due to blunt impact to the head, *Front. Neurol.* 11 (2020) 998, <https://doi.org/10.3389/fneur.2020.00998>. Sep.
- [57] L. Noël, E. Kuhl, Modeling neurodegeneration in chronic traumatic encephalopathy using gradient damage models, *Comput. Mech.* 64 (5) (2019) 1375–1387, <https://doi.org/10.1007/s00466-019-01717-z>. Nov.
- [58] H. Ling, et al., Mixed pathologies including chronic traumatic encephalopathy account for dementia in retired association football (soccer) players, *Acta Neuropathol.* 133 (3) (2017) 337–352, <https://doi.org/10.1007/s00401-017-1680-3>. Mar.
- [59] T.P. Dompier, et al., Incidence of concussion during practice and games in youth, high school, and collegiate American football players, *JAMA Pediatr.* 169 (7) (2015) 659–665, <https://doi.org/10.1001/jamapediatrics.2015.0210>. Jul.
- [60] Z.Y. Kerr, et al., Epidemiologic measures for quantifying the incidence of concussion in national collegiate athletic association sports, *J. Athl. Train.* 52 (3) (2017) 167–174, <https://doi.org/10.4085/1062-6050-51.6.05>. Mar.
- [61] L. Donaldson, M. Asbridge, M.D. Cusimano, Bodychecking rules and concussion in elite hockey, *PLoS One* 8 (7) (Jul. 2013) e69122, <https://doi.org/10.1371/journal.pone.0069122>.
- [62] J.T. Matser, A.G. Kessels, B.D. Jordan, M.D. Lezak, J. Troost, Chronic traumatic brain injury in professional soccer players, *Neurology* 51 (3) (1998) 791–796, <https://doi.org/10.1212/wnl.51.3.791>. Sep.
- [63] A.T. Tysvaer, E.A. Løchen, Soccer injuries to the brain: a neuropsychologic study of former soccer players, *Am. J. Sports Med.* 19 (1) (1991) 56–60, <https://doi.org/10.1177/036354659101900109>. Jan.
- [64] N.J. Cecchi, D.C. Monroe, W.X. Moscoso, J.W. Hicks, D.J. Reinkensmeyer, Effects of soccer ball inflation pressure and velocity on peak linear and rotational accelerations of ball-to-head impacts, *Sports Eng.* 23 (1) (2020) 16, <https://doi.org/10.1007/s12283-020-00331-0>. Sep.
- [65] K. Peek, et al., The effect of ball characteristics on head acceleration during purposeful heading in male and female youth football players, *Sci. Med. Football* 5 (3) (2021) 195–203, <https://doi.org/10.1080/24733938.2021.1897657>. Jul.
- [66] N. Shewchenko, C. Withnall, M. Keown, R. Gittens, J. Dvorak, Heading in football. Part 3: effect of ball properties on head response, *Br. J. Sports Med.* 39 (2005) i33–i39, <https://doi.org/10.1136/bjism.2005.019059>. Suppl 1Aug.